Biophysical Chemistry 180–181 (2013) 10–21

Contents lists available at ScienceDirect

Biophysical Chemistry

journal homepage: http://www.elsevier.com/locate/biophyschem

The helical propensity of KLA amphipathic peptides enhances their binding to gel-state lipid membranes

Ahmad Arouri [a,*], Margitta Dathe [b], Alfred Blume [a]

[a] Institute of Chemistry, Martin-Luther-University Halle-Wittenberg, von-Danckelmann-Platz 4, D-06120 Halle(Saale), Germany
[b] Institute of Molecular Pharmacology, Robert-Rossle-Strasse 10, D-13125 Berlin, Germany

HIGHLIGHTS

- KLA peptides with low helical propensity have high tendency to form beta-structures.
- KLA helical peptides bind more efficiently than beta-structured peptides to gel-state membranes.
- The peptide helical propensity enhances binding to lipid membranes.
- Stoichiometry values from ITC experiments can be used to comment on peptide translocation across membranes.

GRAPHICAL ABSTRACT

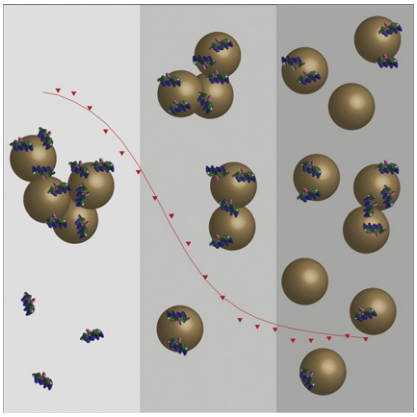

ARTICLE INFO

Article history:
Received 11 April 2013
Received in revised form 17 May 2013
Accepted 18 May 2013
Available online 24 May 2013

Keywords:
Antimicrobial peptide
Isothermal titration calorimetry
Lipid–peptide interaction
Peptide helicity
Structure–activity relationship

ABSTRACT

The role and importance of the conformation of antimicrobial peptides for their binding and incorporation into lipid membranes as well as for their bioactivity are still not well understood. In this paper, we studied the interaction between four cationic alpha-helical KLA peptides, which differ primarily in their helical propensity, and the anionic gel-state lipid DPPG (1,2-dipalmitoyl-*sn*-glycero-3-phosphoglycerol). Of particular interest was the influence of the peptide conformation and membrane surface properties on the electrostatic binding process. Dynamic light scattering (DSL) showed that generally the KLA peptides possess high aggregation power but modest solubilization power. Circular dichroism spectroscopy (CD) spectra revealed that the KLA peptides with the low helical propensity tend to form beta-structures at low lipid/peptide ratios. Differential scanning calorimetry (DSC) thermograms showed that the helical KLA peptides stabilize the DPPG bilayer, whereas the beta-structured peptides induce pronounced membrane perturbations. Isothermal titration calorimetry (ITC) isotherms showed that the helical KLA peptides bind more efficiently to DPPG vesicles than

Abbreviations: FDA, Food and Drug Administration; TFE, Trifluoroethanol; ITC, Isothermal titration calorimetry; DLS, Dynamic light scattering; DSC, Differential scanning calorimetry; CD, Circular dichroism spectroscopy; LUVs, Large unilamellar vesicles; SUVs, Small unilamellar vesicles; MIC, Minimum inhibitory concentration; RBC, Red blood cells; Lys, Lysine; Leu, Leucine; Ala, Alanine; Trp, Tryptophan; PC, Phosphatidylcholine; PE, Phosphatidylethanolamine; PG, Phosphatidylglycerol; DPPC, 1,2-Dipalmitoyl-sn-glycero-3-phosphocholine; DPPE, 1,2-Dipalmitoyl-*sn*-glycero-3-phosphoethanolamine; DPPG, 1,2-Dipalmitoyl-*sn*-glycero-3-phosphoglycerol; POPC, 1-Palmitoyl-2-oleoyl-*sn*-glycero-3-phosphocholine; POPG, 1-Palmitoyl-2-oleoyl-*sn*-glycero-3-phosphoglycerol; L/P, Lipid peptide ratio; T_m, Main phase transition temperature; K_{app}, Apparent binding constant; ΔH^o, Standard enthalpy change; ΔS^o, Standard entropy change, ΔG^o, Standard free energy change; ΔC_p, Constant pressure heat capacity change; N, Stoichiometry.

* Corresponding author at: MEMPHYS-Center for Biomembrane Physics, Department of Physics, Chemistry and Pharmacy, University of Southern Denmark, Campusvej 55, DK-5230, Odense, Denmark. Tel.: +45 6550 3686; fax: +45 6550 4048.
E-mail addresses: arouri@memphys.sdu.dk (A. Arouri), dathe@fmp-berlin.de (M. Dathe), alfred.blume@chemie.uni-halle.de (A. Blume).
URL: http://www.memphys.dk (A. Arouri).

0301-4622/$ – see front matter
http://dx.doi.org/10.1016/j.bpc.2013.05.003

the beta-structured KLA peptides, and that the binding affinity of the peptides is proportional to the peptide helical propensity and membrane negative surface charge. The stoichiometry values (N) deduced from the ITC isotherms suggest that the helical KLA peptides have a higher capacity to translocate the DPPG lipid bilayer. The new data presented in this study demonstrate the flexibility of KLA peptides in adopting various conformations in response to the surrounding and also how the peptide structuring controls the mode of peptide–membrane interaction.

1. Introduction

Bacterial resistance is a growing problem that threatens our ability to treat infections, particularly as it is not adequately compensated by the development of new generations of antibiotics. For instance, 16 new antibiotics were introduced during 1983–1987 as compared with 5 during 2003–2007 [1]. Moreover, of the 13 new antibiotics approved by the Food and Drug Administration (FDA) between 1998 and 2007, only three were with novel mechanisms of action [2]. This calls for new approaches to treat infections that are less prone to induce bacterial resistance. Bacteriophages, bacterial cell wall hydrolases, and antimicrobial peptides are among the most promising candidates [3]. Antimicrobial peptides interact with the lipid components of bacterial membranes, and their non-specific mode of action hampers the development of bacterial resistance. The selective attraction of antimicrobial peptides to bacterial membranes, which contain appreciable amounts of negatively charged lipids like phosphatidylglycerol (PG) and cardiolipin, is furnished by their cationic nature. The peptide amphipathicity is also necessary for its incorporation into lipid membranes [4,5]. It is widely accepted that the final target of antimicrobial peptides is to disrupt the permeability barrier, function, and integrity of bacterial membranes. This may take place by perforating and breaking down the lipid membrane, or interfering with the organization of the lipid species in the membrane via, for instance, peptide-induced lipid demixing, domain formation, and formation of non-lamellar phases [6–15]. The scenario of action depends on the interplay between the peptide macroscopic properties and the composition of the target membrane [6].

KLA peptides are model cationic α-helical peptides that were synthesized to study the structure–activity relationship of antimicrobial peptides [16–19]. The nomenclature and sequences of the KLA peptides used in this study are shown in Table 1, and their properties and activities are shown in Table 2. Except that KLA1 peptide has a slightly lower hydrophobicity, the studied peptides differ only in their helical propensity. The 18-mer KLA peptides posses a nominal charge of +6 provided by five Lys residues and an uncapped N-terminus, whereas the C-terminus is amidated. In an α-helical KLA peptide, the charged residues cover a 90° angle of the peptide interface, whereas the non-polar amino acids (Leu, Ala, Trp) form the hydrophobic part of the amphipathic peptide. The α-helical structure of KLA1 peptide is shown in Fig. 1. Double D-substitution, where two consecutive L-amino acids are replaced with their D-analogues, was utilized to disturb, or sometimes improve, the intrinsic helicity of KLA peptides without affecting other properties. Compared with the all L-peptide KLAL, the double D-substitution in the middle of the KLAL chain pronouncedly disturbed the peptide helicity as in k_9,a_{10}-KLAL and l_{11},k_{12}-KLAL peptides, whereas the double D-substitution at the C-terminus enhanced the peptide helicity, as in k_1, l_2-KLAL peptide [16,19]. Besides the helicity (α), the peptide charge, amphipathicity, hydrophobicity (H), hydrophobic moment (μ) and the hydrophobic/hydrophilic domain ratio (Φ/Ψ) were investigated (see Table 2).

The KLA peptides can adopt different conformations depending on the surrounding and on the experimental conditions. The peptides are unstructured in buffer up to millimolar concentrations, whereas they assume an α-helical structure in trifluoroethanol (TFE) or when added to lipid vesicles. However, the peptides tend to form β-structures at higher peptide concentrations, low lipid to peptide ratios (L/P) or high temperatures [16,20–22]. When bound to 1-palmitoyl-2-oleoyl-*sn*-glycero-3-phosphoglycerol (POPG) vesicles at relatively high L/P ratios (230–500), the order of the peptides according to their helical content is k_1,l_2-KLAL (74%) > KLA1 (54%) > k_9,a_{10}-KLAL (48%) ≥ l_{11},k_{12}-KLAL (47%) (see Table 2). The structuring of the bound peptide is induced predominately by the hydrophobic interaction of the peptide residues with the membrane hydrophobic core, whereas the key role of the positive charge of the peptide is to increase its accumulation on negatively charged lipid membranes [16]. The helical structuring, which induces amphipathicity, enhances the incorporation into lipid membranes as well as the antimicrobial and hemolytic activities of the peptide. This enhancement is caused by the greater disturbance of the lipid headgroups and hydrocarbon chains of lipid membranes [4,23]. The KLA peptides interact strongly with anionic lipid membranes, whereas their affinity towards uncharged membranes of phosphatidylcholine (PC) and phosphatidylethanolamine (PE) is modest [16,21,22,24]. The peptides also exhibit pronounced membrane perturbation and permeabilizing activities [16,24].

In this study, we characterized the electrostatic interaction between a set of KLA peptides and anionic gel-state membranes. Of particular interest was the influence of the peptide conformation and membrane surface properties on the binding process. Anionic large unilamellar vesicles (LUVs) were prepared of 1,2-dipalmitoyl-*sn*-glycero-3-phosphoglycerol (DPPG). Circular dichroism (CD) spectroscopy was utilized to determine the conformation of the peptides bound to DPPG, dynamic light scattering (DLS) was utilized to follow the aggregation of the DPPG-peptide complexes, differential scanning calorimetry (DSC) was utilized to determine the phase behavior of the peptide-bound DPPG bilayers, and isothermal titration calorimetry

Table 1
The nomenclature and sequences of KLA peptides.[a]

Peptide	Sequence
KLA1	KLAL KLAL KAW KAAL KLA-NH_2
k_1,l_2-KLAL	klAL KLAL KAL KAAL KLA-NH_2
k_9,a_{10}-KLAL	KLAL KLAL kaL KAAL KLA-NH_2
l_{11},k_{12}-KLAL	KLAL KLAL KAl kAAL KLA-NH_2

[a] The one letter code is used to give the sequence; K: lysine, L: leucine, A: alanine, W: tryptophan. The capital and small letters are used to show L-amino acids and D-amino acids, respectively.

Table 2
The properties and activities of the studied KLA peptides.[a]

Peptide	H	μ	Helicity (α%)			MIC (μM)		EC_{50} (μM)
			TFE	POPG	DPPG	*E. coli*	*S. epidermidis*	RBC
KLA1	−0.025	0.329	73	54[b]	15[d]	5.2	–	11
k_1,l_2-KLAL	−0.016	0.334	68	74[c]	68[d]	4	4	7
l_{11},k_{12}-KLAL	−0.016	0.334	34	47[c]	7[d]	32	32	540
k_9,a_{10}-KLAL	−0.016	0.334	43	48[c]	2[d]	16	16	56

[a] Adapted from Refs. [16,17,19], except the helicity (α%) values in DPPG which were determined as described in Section 2.3. The helicity values (α%) of the peptides in 50% TFE (v/v) or in POPG were determined in Tris buffer using 10 μM peptide concentration.
[b] L/P = 500.
[c] L/P = 230.
[d] L/P = 10–40.

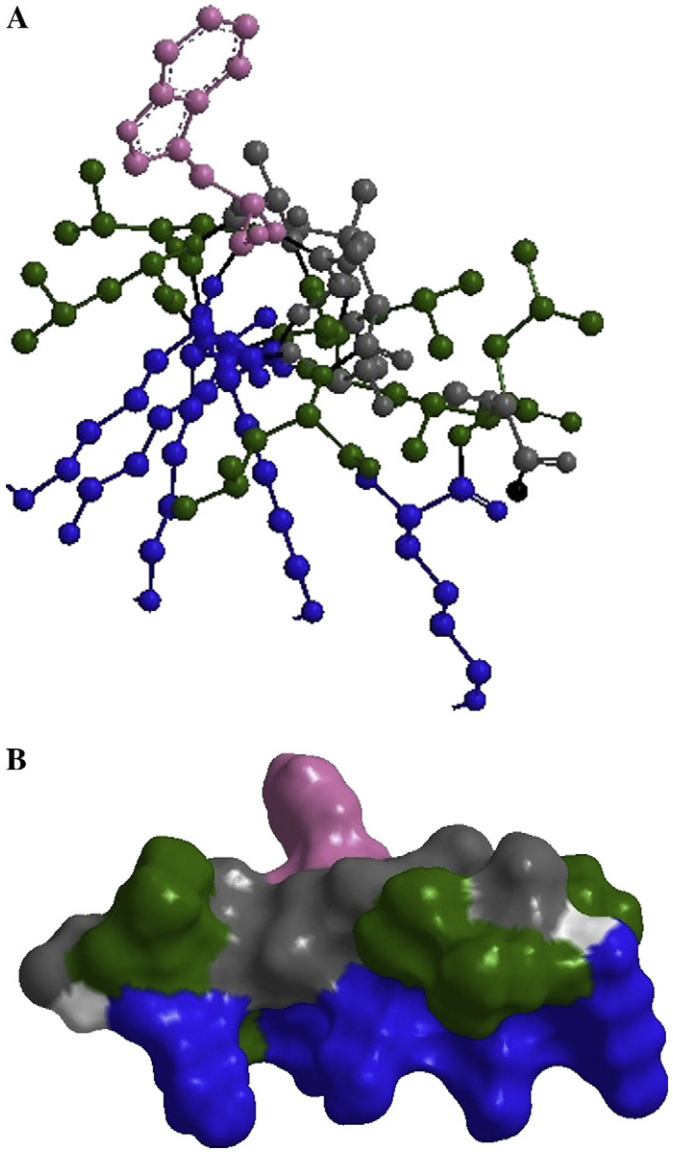

Fig. 1. An illustration showing the amphipathic structure of the helical KLA1 peptide, where the basic amino acids are oriented in one direction and the hydrophobic residues are aligned in the opposite direction. In the side view (A) and the Connolly surface (B), Lys (K) is blue, Leu (L) is green, Ala (A) is gray, Trp (W) is pink, and the backbone is light gray.

(ITC) was utilized to quantify the thermodynamic parameters of the interactions between KLA peptides and DPPG LUVs.

2. Materials and methods

2.1. Materials

KLA1 (KLAL KLAL KAW KAAL KLA-NH_2) and the other D-amino acid analogues (Table 1) were synthesized using the Fmoc technique and purified by reversed phase high performance liquid chromatography RP-HPLC [16] and applied as HCl salt. The peptide solutions were freshly prepared in an aqueous Tris buffer (10 mM Tris/Tris–HCl, 154 mM NaCl, pH 7.4) by weighing the lyophilized samples, dissolving them in buffer, and diluting the samples to the required concentration. The one-letter code is used to give the sequences.

1,2-Dipalmitoyl-*sn*-glycero-3-phosphoglycerol (DPPG), 1,2-dipalmitoyl-*sn*-glycero-3-phosphocholine (DPPC), and 1,2- dipalmitoyl-*sn*-glycero-3-phosphoethanolamine (DPPE) were purchased from Genzyme GmbH, Germany. All lipids were used as received without any further purification or modification. The concentration was calculated from the weight of the dry lipid samples (weight/volume).

Tris, Tris–HCl, NaCl, chloroform, and methanol were purchased from Sigma-Aldrich (Steinheim, Germany).

2.2. Preparation of liposomes

The lipid mixtures were prepared in a chloroform/methanol 2:1 (v/v) mixture, after which the organic solvent was evaporated under vacuum. The liposomes were freshly prepared using the Avanti Mini Extruder (Avanti Polar Lipids), where the lipid dispersions were extruded 15 times through two 100 nm diameter polycarbonate filters at a temperature higher than the phase transition temperature of the lipid or lipid mixture. The lipid samples were prepared in an aqueous Tris buffer (10 mM Tris/Tris–HCl, 154 mM NaCl, pH 7.4).

2.3. Circular dichroism spectroscopy (CD)

Far UV-CD spectra were obtained using Jasco J810 spectropolarimeter equipped with a Peltier device. The peptides (25–100 μM) and the extruded lipid vesicles (1 mM) were prepared in an aqueous Tris buffer and mixed in a 0.1 cm cuvette to achieve an L/P ratio of 10 to 40. Thereafter, 10 to 20 accumulations of the CD spectra were recorded in the range of 190–260 nm. The spectra were corrected from the circular dichroism and differential scattering due to lipid vesicles and then averaged and smoothed. The peptide helicity [α] was determined from the mean residue ellipticity $[\Theta]_{MRW}$ at 222 nm according to the relation $[\Theta]_{222} = -30{,}300\,[\alpha] - 2340$ [25].

2.4. Dynamic light scattering (DLS)

The dynamic light scattering measurements were performed by means of ALV-NIBS/HPPS high performance particle sizer (ALV-Laser Vertriebsgesellschaft m.b.H., Langen, Germany). The system is equipped with a HeNe laser of 3 mW output power at a wavelength of 632.8 nm, a backscattering arrangement (the scattering angle is 173°) and an avalanche photodiode as a detection system. The temperature of the sample compartment can be regulated by a software-controlled Peltier device. The titration experiments were carried out by 10–50 μl multi-step titrations of 1 mM vesicle suspension into 500 μl of 5–10 μM peptide solution (starting volume and concentration) placed in a disposable 1 cm poly(methyl methacrylate) (PMMA) cuvette (Brand GmbH + Co. KG, Wertheim, Germany). After the addition of the liposomes, the sample in the cuvette was equilibrated for one minute after which the autocorrelation function was recorded for 180 s (6 × 30 s), and the autocorrelations were then averaged. The data were fitted and analyzed using the ALV-5000/E/EPP software (Version 3.0) supplied with the instrument, which is based on CONTIN software package [26] that uses Laplace transforms for the inversion of the autocorrelation function. The normalized unweighted particle size distributions, which correlate the particle size with its respective scattering intensity, were determined using the linear regularized fit model.

2.5. Differential Scanning Calorimetry (DSC)

The DSC measurements were carried out using VP-DSC from MicroCal™ Inc. (Northampton, MA). The lipid–peptide mixtures with the desired ratio were freshly pre-mixed prior to the DSC experiments. The final lipid and peptide concentrations were 1–2 mM and 5–200 μM, respectively. The samples were degassed for 10 min before being loaded. A scanning rate of 1 °C min^{-1} was applied. The reference cell was filled with buffer. Several heating and cooling scans were performed to ensure the reproducibility of the thermograms.

2.6. Isothermal titration calorimetry (ITC)

The ITC measurements were carried out using a VP-ITC from MicroCal™, Inc. (Northampton, MA). Prior to each experiment, the sample cell and the syringe were washed with freshly distilled water, rinsed using chloroform/methanol 2:1 (v/v), and dried using an air stream. The reference cell was filled with degassed water. The 1.4 ml reaction cell was loaded with the peptide solution (5 μM), whereas the injection syringe (nominal volume 250 μl) was filled with the vesicle suspension with a concentration of 500 μM. The instrument was equilibrated at a temperature 5 °C below the experimental temperature with an initial delay of 60 s. The reference power and the filter were set to 10 μcal s^{-1} and 2 s, respectively. Each experiment was carried out in duplicates or more. After the point of the first injection was discarded, the titration curves were analyzed using the one-site binding model in the ORIGIN® software provided with the calorimeter. In this model, and when titrating lipid vesicles to peptides, the lipid molecules are treated as ligands and the peptide is assumed to have *n* number of independent and equivalent binding sites.

3. Results

3.1. Circular dichroism spectroscopy (CD)

CD spectroscopy was utilized to determine the conformation of KLA peptides bound to DPPG LUVs at low L/P ratios (10–40). As the CD spectra in Fig. 2 show, the k_1,l_2-KLAL peptide preserves to a large degree its helical conformation (68%, see Table 2), as evident by the negative ellipticity at 207 and 222 nm and the positive CD band below 200 nm. In contrast, the helical content of the KLA1 peptide drops to 15%, whereas the peptides with the lower intrinsic helicity l_{11}, k_{12}-KLAL and k_9,a_{10}-KLAL assume β-strands and their helical content is only 7% and 2%, respectively. Unpublished Fourier transform infrared spectroscopy (FT-IR) data propose that the KLA peptides form β-aggregates rather than normal β-strands [27]. It is possible that the helical content of the peptides is slightly underestimated due to peptide-induced vesicle aggregation and precipitation (see Section 3.2), which could increase the light scattered off the samples as well as decrease the peptide available for the light beam. We refrained from the deconvolution of our CD data to determine the fractions of the different conformations due to the lacking of proper reference data, albeit the presence of robust algorithms.

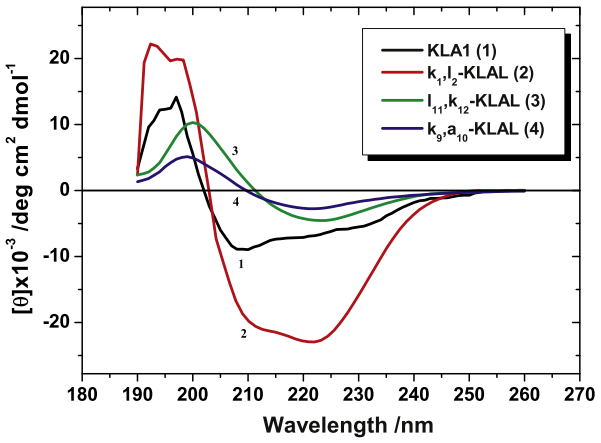

Fig. 2. CD spectra of KLA peptides (25–100 μM) in DPPG suspension (~50 nm radius, 1 mM, L/P 10 to 40) at 20 °C. The samples were prepared in Tris buffer (10 mM Tris, 154 mM NaCl, pH 7.4).

3.2. Dynamic light scattering (DLS)

DLS serves as a potent tool to investigate interactions of membrane-active agents with lipid vesicles, and such interactions are usually associated with altering the size and shape of the vesicles [28,29]. As a result, one obtains a direct evidence of the ligand affinity and selectivity. We utilized DLS to monitor the influence of KLA peptides on the average size of extruded DPPG and DPPC vesicles. To mimic ITC experiments, lipid vesicles were titrated into peptide solutions in the cuvette. The average size distribution of the lipid vesicles without peptide was controlled prior to each experiment. This procedure helps to achieve low L/P ratios after the first injection of lipid vesicles. However, this will also cause the aggregation of lipid vesicles hindering the detection of any possible changes in the size of individual lipid vesicles, for instance due to vesicle solubilization. The further additions of vesicles continuously will increase the lipid fraction in the system until the aggregation capacity of the peptides is exceeded, which will drive the dissociation of the aggregates. As a result, it will be possible to observe the size distribution of the individual vesicles and see the effect of low L/P ratios achieved at the beginning of the titration.

Fig. 3 shows the unweighted radius size distribution of extruded DPPG (54 nm average radius) without peptide and of DPPG titrated into KLA1 (high helical propensity) and k_9,a_{10}-KLAL (low helical propensity) solutions. The unweighted size distribution, also known as intensity-weighted, shows the intensity of the light scattered off the particles as a function of particle size. The titrations were performed at 25 °C at which DPPG is in gel state. At an L/P ratio of 2, a broad radius size distribution centred ~320 nm is observed with both peptides. The further addition of DPPG vesicles causes a peak splitting showing two populations with distinct average size distributions. Upon increasing the L/P ratio, the larger structures continue to grow, whereas the smaller structures decompose into, most probably, individual vesicles. At and above an L/P of 20, the position of the two peaks remains unaltered whereas their intensity keeps changing upon the addition of vesicles in favor of the peak belonging to the individual vesicles. Since the intensity of the scattered light is usually higher for larger particles, the unweighted distribution function underestimates the number of smaller particles. One can conclude therefore that only few aggregates are present in the sample at the end of the titration (high L/P).

At an L/P ≥ 20, the DPPG-KLA1 structures (~1200 nm) are larger than the structures with k_9,a_{10}-KLAL (~600 nm) suggesting that the aggregation capacity of KLA1 exceeds that of k_9,a_{10}-KLAL. At

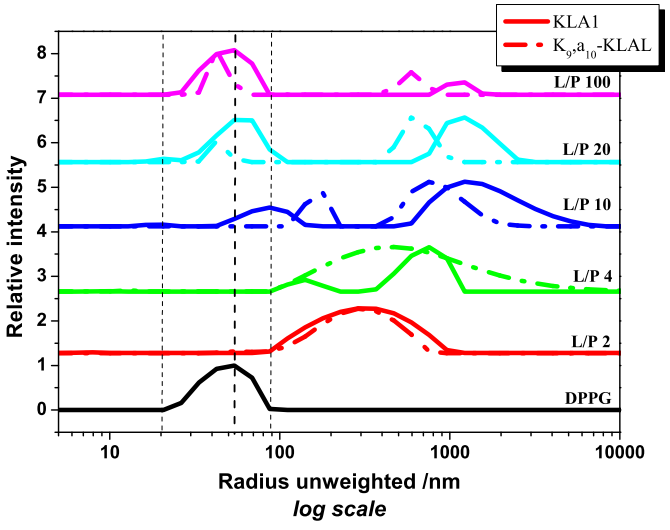

Fig. 3. Unweighted distribution of hydrodynamic radii obtained from DLS measurements of DPPG vesicles (1 mM, ~54 nm average radius) before and after multi-step additions to KLA1 and k_9,a_{10}-KLAL solutions (500 μl, 10 μM) at 25 °C. The samples were prepared in Tris buffer (10 mM Tris, 154 mM NaCl, pH 7.4).

temperatures higher than the phase transition temperature of DPPG (>41 °C) the aggregation power of the peptides is reduced (data not shown). In the titrations with DPPC, the peptides barely affect the size distribution of DPPC vesicles (data not shown).

The origin of the large DPPG-peptide structures cannot be disclosed by DLS experiments; whether they are aggregated or fused vesicles. However, the generally slow kinetics of peptide-induced vesicle fusion (>1 h [30]) as well as the fact that the large structures observed with DLS dissociate at high L/P ratios suggest that these large structures are mainly aggregated DPPG vesicles. The self-association of DPPG vesicles can be driven by peptide molecules that bridge between two or more vesicles and/or by peptide–peptide interactions between peptide molecules bound to DPPG vesicles.

3.3. Differential scanning calorimetry (DSC)

A fully hydrated DPPG bilayer undergoes a pretransition (T_{pre}) from lamellar gel $L_{\beta'}$ to ripple gel $P_{\beta'}$ at ~ 33 °C and a main transition (T_m) to L_α at ~ 41 °C. As shown in Fig. 4(A–D), the KLA peptides supress the pretransition of DPPG, particularly at high peptide contents, and pronouncedly alter its main phase transition.

The interaction of KLA1 with DPPG (see Fig. 4(A)) decreases the enthalpy and cooperativity of the main phase transition in a concentration dependent manner. The effect on T_m is modest at L/P ratios of 200 to 20, whereas the phase transition is significantly broadened and T_m is reduced to ~39 °C at an L/P of 10. In contrast, k_1,l_2-KLAL peptide (see Fig. 4(B)) apparently induces the formation of two domains; a k_1, l_2-KLAL-poor domain with a transition temperature (~40 °C) slightly lower than T_m of unbound DPPG and a k_1,l_2-KLAL-rich domain with a higher transition temperature (~42 °C). The ratio between the two domains is regulated by the peptide content (L/P ratio). Again, at an L/P of 10 only a broad peak with very low intensity can be observed. The peptides with the lowest helical propensity, i.e. l_{11},k_{12}-KLAL (Fig. 4(C)) and k_9,a_{10}-KLAL (Fig. 4(D)), decrease T_m by ~1 °C at an L/P of 200, whereas the peak position at the other L/P ratios is similar to unbound DPPG. At low L/P ratios, the l_{11},k_{12}-KLAL and k_9,a_{10}-KLAL peptides pronouncedly suppress the enthalpy and cooperativity of DPPG main transition, which is almost abolished at an L/P of 10.

As the DSC thermograms reveal, the peptide with the highest helicity k_1,l_2-KLAL shows a strong electrostatic interaction with DPPG vesicles, as the peptide stabilizes the DPPG bilayer and induces domain formation, particularly at high L/P ratios. On the other side, KLA1 and more considerably l_{11},k_{12}-KLAL and k_9,a_{10}-KLAL destabilize the DPPG bilayer decreasing T_m and the transition enthalpy and cooperativity. This behavior is primarily due to the deep burial of the hydrophobic moieties of the peptides into the core of DPPG bilayers and to the consequent perturbation of the acyl chain packing.

3.4. Isothermal titration calorimetry (ITC)

3.4.1. Interaction of KLA peptides with DPPG LUVs

The ITC isotherms and their fits for the binding of the four peptides to DPPG extruded LUVs (~50 nm radius) measured at 15 °C are shown in Fig. 5 and the thermodynamic parameters are listed in Table 3.

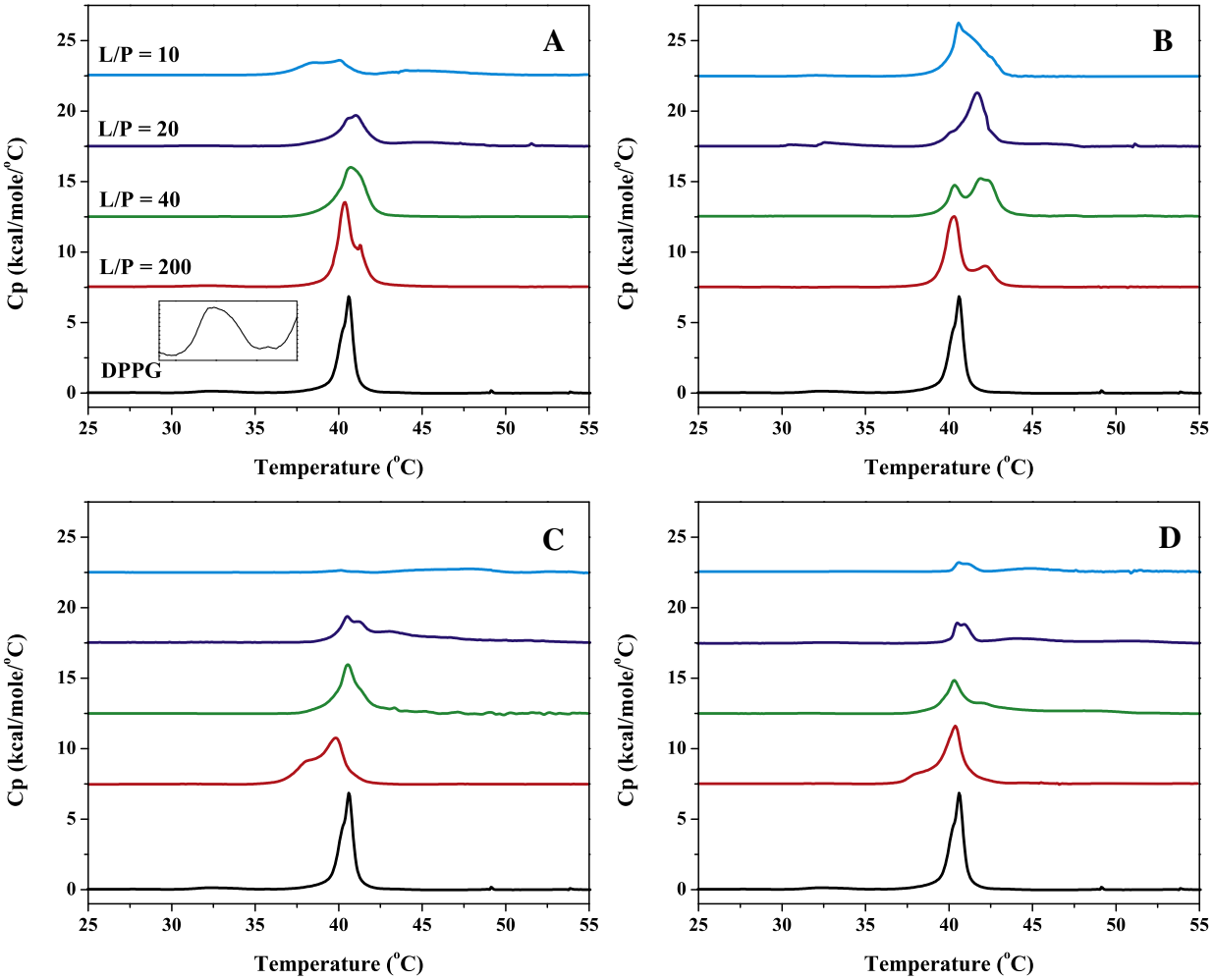

Fig. 4. First heating DSC curves of DPPG LUVs (2 mM) before (black line) and after the addition of (A) KLA1, (B) k_1,l_2-KLAL, (C) l_{11},k_{12}-KLAL and (D) k_9,a_{10}-KLAL peptides with L/P ratios of 200, 40, 20 and 10. The inset in A if a magnification of the DPPG pre-transition. The samples were prepared in Tris buffer (10 mM Tris, 154 mM NaCl, pH 7.4).

The dilution enthalpy of extruded DPPG LUVs titrated into 10 mM Tris buffer (154 mM NaCl, pH 7.4) is 250–350 cal mol^{-1} at 15 °C.

The interactions are entropy driven, with favorable positive TΔS°, compensated by a moderate endothermic contribution with unfavorable positive ΔH°. The apparent binding affinity (K_{app}) of KLA peptides to DPPG correlates well with their helical propensity, and the decrease in K_{app} is almost entirely of entropic origin. As shown in Table 3, K_{app} of k_1,l_2-KLAL, the peptide with the highest helical propensity, is 1.16×10^6 M^{-1} at 15 °C and 154 mM NaCl, which is one order of magnitude higher than K_{app} of k_9,a_{10}-KLAL, the peptide with the lowest helical propensity. For the peptides k_1,l_2-KLAL, KLA1 and l_{11},k_{12}-KLAL, the favorable TΔS° decreases with the helicity while the endothermic ΔH° increases. k_9,a_{10}-KLAL shows the lowest K_{app}, ΔH° and TΔS° values among all KLA peptides. The decrease in the K_{app} values with helicity is not dramatic, possibly because the KLA peptides with the low intrinsic helicity can form β-structures at low L/P ratios, i.e. at the beginning of the ITC titration, which also can bind to DPPG vesicles. However, the decrease in K_{app} indicates that the helical KLA peptides bind more efficiently to DPPG vesicles than β-structured KLA peptides.

3.4.2. Influence of surface charge density

We tested the effect of the membrane negative surface charge density on the binding profiles of the peptides via mixing DPPG with DPPC or DPPE at various molar ratios. Fig. 6 shows the ITC titrations for the interaction of KLA1 with DPPG, DPPC, DPPE and the mixed membranes DPPG/DPPC and DPPG/DPPE with varying molar ratios. The measured isotherms are composed of an exothermic dilution enthalpy overcompensated in the beginning by an endothermic part associated with the binding process. The binding process and the associated endothermic part are found to be highly dependent on the negative charge content of the bilayer. Reducing the DPPG fraction to 50% in both mixed systems leads to titration curves without significant changes in the heat effects indicating negligible binding under our experimental conditions.

The KLA peptides interact only weakly with uncharged lipids [16,17,24]. Binding isotherms derived from CD spectra were utilized to determine K_{app} of binding to 1-palmitoyl-2-oleoyl-*sn*-glycero-3-phosphocholine (POPC) and POPG/POPC 1:3 vesicles and the values were found in the order of 10^3 and 10^4 M^{-1}, respectively [16]. Due to these low apparent binding constants and a small ΔH° value, the binding cannot be detected by ITC. In an earlier study, we had observed similar effects, as it was also not possible to detect the weak interactions between KLA peptides and uncharged monolayers using Langmuir monolayer experiments [21].

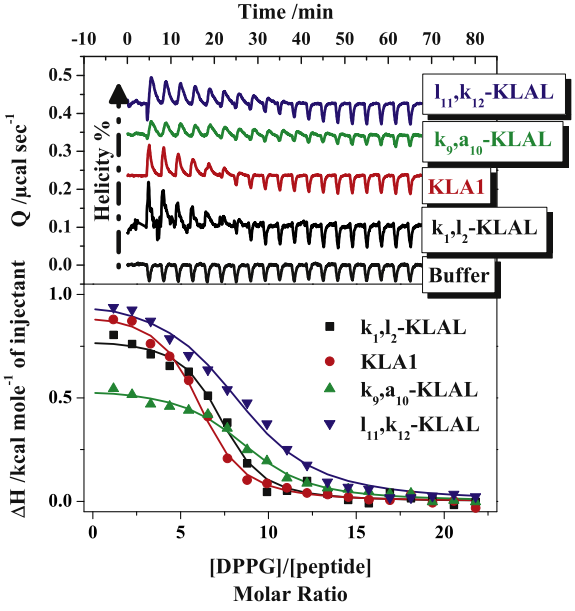

Fig. 5. The experimental power signals (top) and the integrated peaks (bottom) as a function of DPPG/peptide ratio. The solid lines are the hypothetical fits of the integrated peaks. In the experiments, DPPG LUVs (500 μM) in the syringe were titrated into KLA peptides (5 μM) or buffer in the reaction cell at 15 °C. The samples were prepared in Tris buffer (10 mM Tris, 154 mM NaCl, pH 7.4).

The thermodynamic parameters for the interactions of k_1,l_2-KLAL and KLA1 with DPPG/DPPC 3:1 and DPPG/DPPE 3:1 mixed membranes are presented in Table 3. We refrained from fitting the binding isotherms of k_9,a_{10}-KLAL and l_{11},k_{12}-KLAL due to the low reaction enthalpy with the mixed membranes. The binding affinities and energies obtained for DPPG/DPPC 3:1 and DPPG/DPPE 3:1 are comparable, however, slightly lower than DPPG. Again, the proportionality between the helical propensity and the binding affinity is also observed in both mixed systems. In principle and since the interactions of the peptides are driven by electrostatics, reducing the DPPG fraction will lower the surface concentration of the peptides. However, the decrease in the surface charge density in the membrane might give the peptide the opportunity to pack better on the vesicle surface [31] and to sink deeper in the membrane [32].

3.4.3. Influence of salt concentration

Due to the charge screening effects of salt ions, inspecting the influence of ionic strength on biomolecular interactions is a common procedure to validate the electrostatic contribution to the binding process. For electrostatically driven associations, a substantial inverse-dependence of the binding affinity on salt concentration was established, which was predominately of entropic origin [33–36]. In fact, the interaction of charged peptides with the uncharged POPC was found to be weaker at high salt concentrations [37]. In contrast, peptide–protein interactions of hydrophobic origin were barely affected by increasing the salt concentration [38].

We performed ITC titrations of DPPG LUVs into KLA1 at 15 °C using 154, 300, 500 and 1000 mM NaCl. A comparison between the recorded isotherms (see Fig. 7(A)) shows the strong influence the salt concentration has on the binding constant and the reaction enthalpy, since no binding could be detected at 1000 mM NaCl. The effect of varying the NaCl concentration on the binding parameters (ΔH°, TΔS° and ΔG°) is shown in Fig. 7(B) and the numerical values are listed in Table 3. Increasing the NaCl concentration efficiently reduces K_{app}, the endothermic ΔH°, and TΔS°.

According to the equation $\log K = \log K_T - z\log[Na^+]$, plotting the experimental $\log K_{app}$ as a function of $\log[Na^+]$ should be linear. The slope z is the amount of Na^+ released upon the binding to one DPPG molecule, whereas the Y-intercept represents $\log K_T$. K_T is the binding constant at 1 M Na^+ concentration; commonly known as $K_{nonionic}$, since at this salt concentration the electrostatic binding is highly suppressed [34,39]. In these calculations, the ions coming from the DPPG and peptide samples are not taken into consideration since their amounts are negligible in comparison to the salt concentration in buffer. The binding of KLA1 peptide to one DPPG molecule releases in average 1.4 Na^+ ions, whereas the nonionic binding constant K_T is 6.3×10^4 M^{-1}. This analysis of the influence of NaCl concentration points again to the importance of the electrostatic attraction for driving the binding of KLA peptides to negatively charged lipid vesicles. Nonetheless, the hydrophobic effects in the interaction process should not be affected.

3.4.4. Influence of temperature

To further characterize the interaction of KLA1 with DPPG vesicles, ITC titrations were carried out over the temperature range of 5–50 °C. The binding isotherms measured at 5–25 °C and their fits are shown in Fig. 8(A). The results show that with increasing temperature, the reaction enthalpy becomes more endothermic and the saturation occurs at lower DPPG/KLA1 molar ratios (discussed later).

Table 3
The thermodynamic parameters of the interactions of KLA peptides with lipid vesicles at different conditions.[a]

Peptide	Lipid	[NaCl]/mM	T/°C	N	$K_{app} \times 10^{-5}/M^{-1}$	ΔH°/kcal mol^{-1}	TΔS°/kcal mol^{-1}	ΔG°/kcal mol^{-1}
k_1,l_2-KLAL	DPPG	154	15	7.6 ± 0.1	11.6 ± 2.3	0.81 ± 0.02	8.80 ± 0.09	−7.99 ± 0.10
KLA1[b]	DPPG	154	15	6.4 ± 0.1	8.8 ± 1.6	0.91 ± 0.02	8.75 ± 0.07	−7.84 ± 0.10
l_{11},k_{12}-KLAL	DPPG	154	15	8.5 ± 0.2	3.6 ± 0.6	0.97 ± 0.03	8.28 ± 0.06	−7.31 ± 0.09
k_9,a_{10}-KLAL	DPPG	154	15	9.1 ± 0.5	2.6 ± 0.4	0.78 ± 0.07	7.91 ± 0.04	−7.13 ± 0.09
k_1,l_2-KLAL	DPPG/DPPC 3:1	154	15	16.6(12.5) ± 0.3	6.3 ± 2.1	0.81 ± 0.02	8.45 ± 0.14	−7.64 ± 0.16
KLA1	DPPG/DPPC 3:1	154	15	11.4(8.6) ± 0.1	5.7 ± 0.8	0.58 ± 0.01	8.16 ± 0.06	−7.59 ± 0.07
k_1,l_2-KLAL	DPPG/DPPE 3:1	154	15	10.3(7.7) ± 0.2	7.4 ± 2.6	1.16 ± 0.04	8.89 ± 0.14	−7.73 ± 0.17
KLA1	DPPG/DPPE 3:1	154	15	9.0(6.8) ± 0.3	5.3 ± 1.4	0.66 ± 0.03	8.20 ± 0.11	−7.54 ± 0.14
KLA1	DPPG	154	5	11.7 ± 0.3	3.9 ± 1.0	0.66 ± 0.02	7.77 ± 0.10	−7.11 ± 0.13
KLA1	DPPG	154	10	9.6 ± 0.1	9.9 ± 1.6	0.84 ± 0.01	8.60 ± 0.07	−7.76 ± 0.08
KLA1[b]	DPPG	154	15	6.4 ± 0.1	8.8 ± 1.6	0.91 ± 0.02	8.75 ± 0.07	−7.84 ± 0.10
KLA1	DPPG	154	20	5.6 ± 0.1	6.3 ± 0.8	1.02 ± 0.02	8.79 ± 0.05	−7.77 ± 0.07
KLA1	DPPG	154	25	3.1 ± 0.1	2.9 ± 0.5	1.74 ± 0.10	9.18 ± 0.01	−7.44 ± 0.09
KLA1[b]	DPPG	154	15	6.4 ± 0.1	8.8 ± 1.6	0.91 ± 0.02	8.75 ± 0.07	−7.84 ± 0.10
KLA1	DPPG	300	15	8.8 ± 0.3	2.8 ± 0.6	0.58 ± 0.02	7.76 ± 0.09	−7.18 ± 0.11
KLA1	DPPG	500	15	5.5 ± 0.5	1.7 ± 0.7	0.37 ± 0.05	7.27 ± 0.14	−6.90 ± 0.18

[a] The peptides are ordered according to their helicity in DPPG (see Table 2).
[b] Rows were repeated to ease comparison. *N* in parenthesis shows N values per DPPG molecules. Each experiment was carried out in duplicates or more. The titration curves were analyzed using the "one- site" binding model provided by ORIGIN® software in order to determine the apparent binding constant (K_{app}), the binding enthalpy (ΔH°) and the lipid/peptide binding stoichiometry (N). The standard free energy (ΔG°) and entropy (ΔS°) of the binding were calculated using the standard equations $\Delta G^\circ = -RT\ln K_{app}$ and $\Delta S^\circ = (\Delta H^\circ - \Delta G^\circ)/T$, respectively.

Interesting ITC isotherms were obtained at 30 and 35 °C (see Fig. 8(B)). They show an endothermic process at low DPPG/KLA1 molar ratios, which disappears at a molar ratio of ~6 until another exothermic event starts above the DPPG/KLA1 molar ratio of ~12. As discussed earlier (Section 3.3), the DSC thermograms reveal that the acyl chain packing of DPPG bilayers is pronouncedly perturbed by the binding of KLA peptides. We propose that at temperatures ≥30 °C and during the first part of the ITC titration at an L/P < 6 (equimolar lipid–peptide charge ratio), a peptide-induced gel to fluid phase transition of DPPG takes place (endothermic) due to the presence of excess KLA1. The further titration of DPPG vesicles into the peptide solution will continuously cause a peptide redistribution, which will decrease the local surface peptide concentration. Eventually, above the molar ratio of 12 (full coverage of the outer leaflet) this phenomenon will be reversed, which will be accompanied by the release of heat. Increasing the temperature from 30 to 35 °C enhances the endothermic peptide-induced phase transition and consequently the exothermic event at the end of the titration. This behavior does not appear for the interaction with fluid DPPG at 50 °C (see Fig. 8(B)), where a barely detectable enthalpy change is seen. This supports our interpretation for this phenomenon.

The temperature dependence of the thermodynamic parameters (ΔH°, TΔS°, and ΔG°), which were acquired by fitting the 5–25 °C isotherms (see Fig. 8(A)) is shown in Fig. 9 and the values are listed in Table 3. The binding affinity at 5 and 10 °C are 3.9×10^5 and 9.9×10^5 M^{-1}, respectively, whereas it is slightly reduced to 2.9×10^5 M^{-1} at 25 °C. The unfavorable ΔH° and the favorable

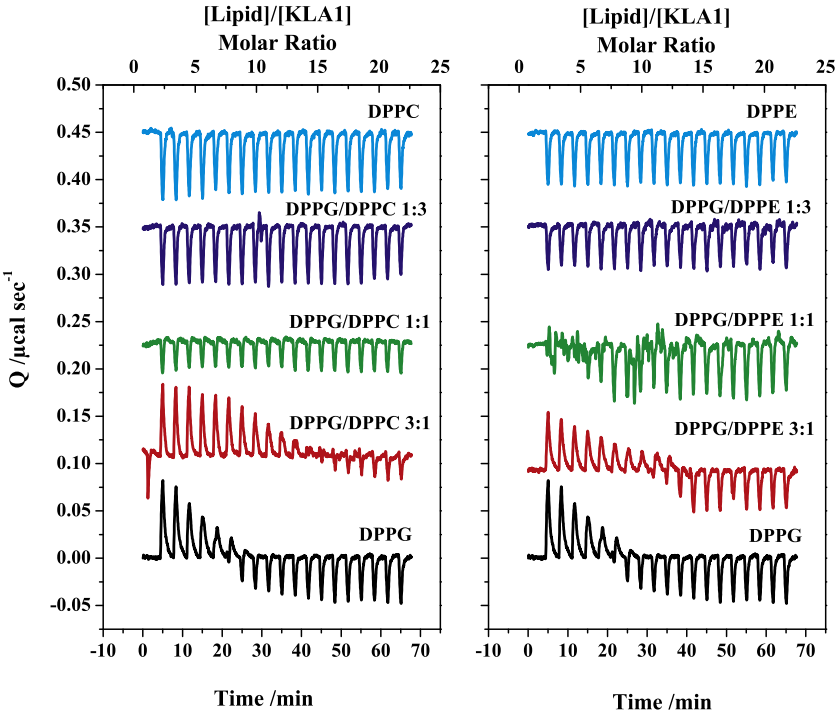

Fig. 6. The experimental power signals of the binding of KLA1 (5 μM) to DPPG/DPPC (left) and DPPG/DPPE (right) LUVs (total lipid concentration 500 μM) as well as to the single components (500 μM) at 15 °C. The samples were prepared in Tris buffer (10 mM Tris, 154 mM NaCl, pH 7.4).

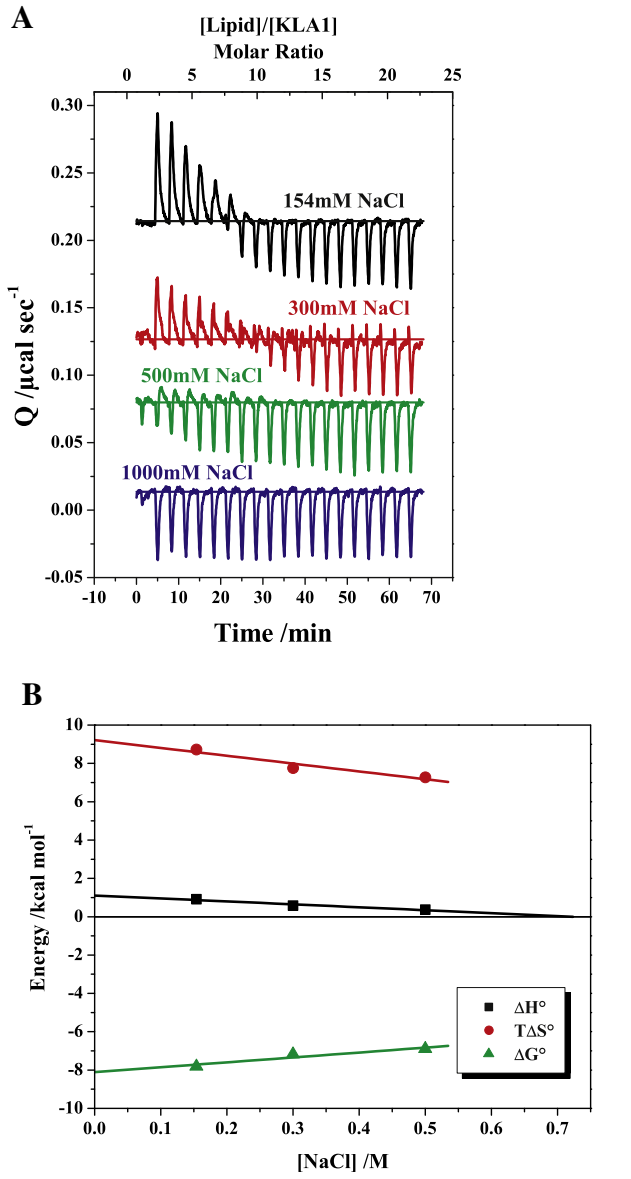

Fig. 7. (A) The experimental power signals of the binding of KLA1 (5 μM) to DPPG LUVs (500 μM) at different NaCl concentrations (154 to 1000 mM) at 15 °C. The samples were prepared in Tris buffer (10 mM Tris, 154 mM NaCl, pH 7.4). (B) The salt concentration dependence of the thermodynamic parameters ΔH°, TΔS° and ΔG° for the binding of KLA1 to DPPG LUVs at 15 °C.

TΔS° of the binding process are slightly increased by increasing the temperature, yet, ΔG° is barely altered due to the known enthalpy–entropy compensation.

The slope of the temperature dependence of ΔH° (5–25 °C) can be used to calculate the change in molar heat capacity (ΔC_p), assuming a temperature-independent ΔC_p. A ΔC_p value of +46.8 cal mol^{-1} K^{-1} was determined. Though it remains difficult to determine the origin of the positive ΔC_p, it is obvious that it is related to some processes that take place only with DPPG in the gel phase. We anticipate that it is due to the temperature enhanced peptide-induced perturbations and fluidization of the lipid hydrocarbon chains.

3.4.5. Stoichiometry of binding

The stoichiometry (N) of binding can be obtained directly from the employed fits, namely from the molar ratio at the inflection point of the ITC curve. The N values, in our case presented as a DPPG/peptide ratio, can be used to estimate the extent of the molecular interactions

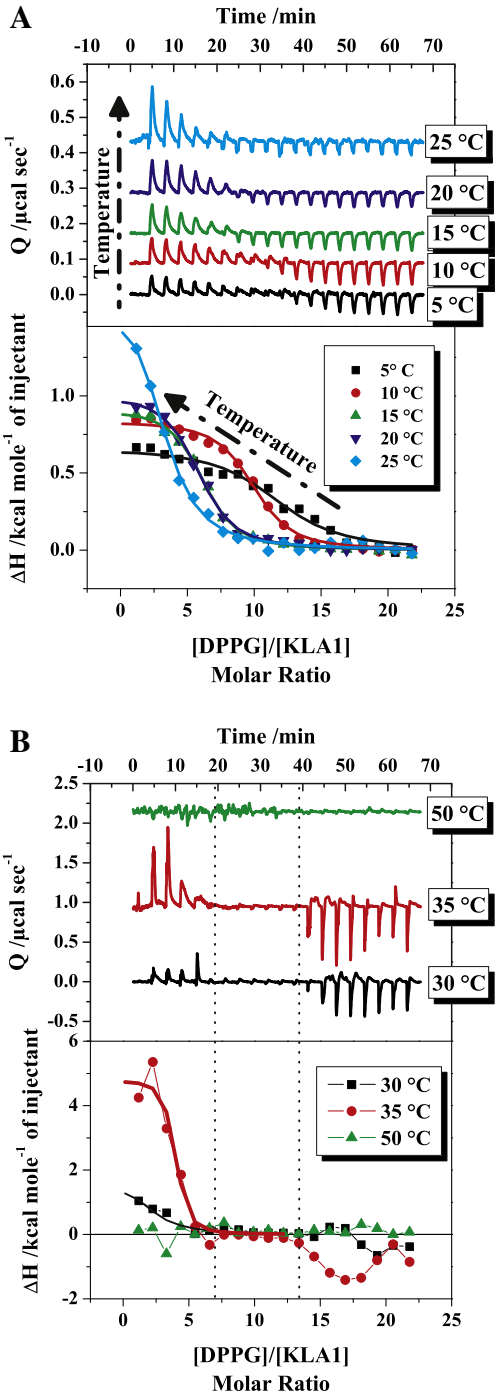

Fig. 8. (A), (B) The experimental power signals (top) and the integrated peaks (bottom) as a function of DPPG/KLA1 ratio. The solid lines (A) are the hypothetical fits of the integrated peaks. In the experiments, DPPG LUVs (500 μM) in the syringe were titrated into KLA1 peptide (5 μM) in the reaction cell at temperatures of 5 to 25 °C (A) and of 30 to 50 °C (B). The samples were prepared in Tris buffer (10 mM Tris, 154 mM NaCl, pH 7.4).

between DPPG and the peptides. For instance, since liposomes are composed of two leaflets, the peptides need to translocate the lipid bilayer to interact with the inner leaflet. If the peptide can translocate the lipid bilayer, the peptide in the cell will be "consumed" sooner as it will bind to two leaflets, which will decrease the N value. Also, peptide as well as liposome aggregation can trap peptide molecules and hinder their interaction with lipids, which will also "consume" the peptide sooner and result in a lower N value.

In contrast to the highly curved small unilamellar vesicles (SUVs) where the outer leaflet contains around 60% of the lipid molecules,

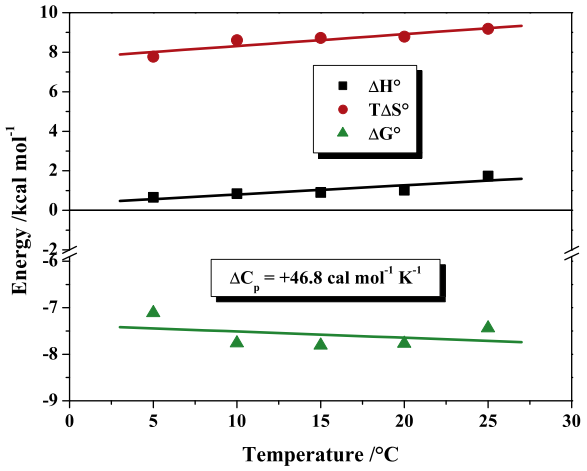

Fig. 9. The temperature dependence of the thermodynamic parameters ΔH°, TΔS° and ΔG° for the binding of KLA1 to DPPG LUVs. The linear temperature dependence of ΔH° was linearly fitted to determine the change in specific heat capacity ΔC_P.

the lipids in LUVs used in our study are almost equally distributed in both leaflets. The KLA peptides have a nominal charge of ~+6 due to five Lys residues and an uncapped N-terminus that is partially charged at neutral pH. Although the effective charge of KLA peptides can be lower than the nominal charge, as reported for some other peptides [32,33,40], the stoichiometry values obtained from the ITC titrations support the assumption that the effective charge of KLA peptides is close to the nominal one.

Since the interaction of KLA peptides with DPPG is electrostatically driven and assuming that the peptides can escape the vesicle aggregates and freely redistribute to the newly added vesicles, as suggested by the DLS data, a DPPG/peptide stoichiometry of 12 will indicate that the peptide binds exclusively to the outer leaflet of DPPG vesicles. On the other hand, a DPPG/peptide stoichiometry of 6 will indicate that the peptide can translocate the lipid bilayer and interact with the inner leaflet of the vesicles as well. Due to the complex nature of interactions with amphipathic peptides, the stoichiometry may deviate from ideality depending on effects like charge screening, steric hindrance, and the formation of lipid-peptide suprastructures.

Interestingly, the stoichiometry values (listed in Table 3) for the interactions of the peptides with DPPG at 15 °C are lower than 12, namely ~7 for the peptides with the higher helical propensity (KLA1 and k_1,l_2-KLAL) and ~9 for the peptides with the lower helical propensity (k_9,a_{10}-KLAL and l_{11},k_{12}-KLAL). These stoichiometry values suggest that either the peptides can translocate the DPPG bilayer and interact with the membrane inner leaflet or that the peptides cannot totally escape the lipid aggregates and cannot freely redistribute in the reaction cell. The generally lower stoichiometry values of KLA1 and k_1, l_2-KLAL may indicate their higher ability to translocate the DPPG bilayer and/or their stronger binding to DPPG vesicles (i.e. less redistribution). The higher stoichiometry values of k_9,a_{10}-KLAL and l_{11},k_{12}-KLAL can be attributed to their formation of β-aggregates, which do not only bind less efficiently to lipid membranes but also cannot form structural pores.

The change in the binding stoichiometry with temperature can also be utilized to comment on the interactions with the DPPG lipid vesicles over the studied temperature range. As shown in Table 3, K_{app} slightly decreases with temperature, whereas N pronouncedly decreases with temperature from ~12 at 5 °C to ~3 at 25 °C. This can indicate that increasing the temperature ($T < T_m$) enhances the permeability of the vesicles probably caused by the reduction in lipid chain packing and the formation of defects due to the expansion of the membrane. In similar systems, temperature was reported to ease and accelerate the translocation across lipid membranes [41,42].

Interestingly, the stoichiometry values of interactions with lipid vesicles are not strictly reproducible as in the case of, for instance, ligand–protein binding [38]. Therefore, the N values shown in this study are averages of broader stoichiometry ranges.

4. Discussion and conclusions

Several studies inspected the correlation between the structural properties of antimicrobial peptides and their antimicrobial activity and selectivity, based on the fact that the activity is determined by the macroscopic properties of the peptides rather than the exact sequence or order of amino acids [4,5,15,43,44]. Despite the large amount of experimental data available, the influence and importance of the conformation of antimicrobial peptides for their binding and incorporation into lipid membranes are still not well-understood [15]. In this study, we focus on the electrostatic binding of several cationic KLA peptides, which primarily differ in their helical propensity, to anionic gel-state lipid membranes. Although biological membranes are fluid in nature, gel-state membranes are more useful to monitor the events associated with electrostatic binding, since gel-state liposomes behave more like "solid spheres" as compared with fluid liposomes, and therefore processes subsequent to the initial binding, like peptide reorientation in the membrane and the formation of peptide–lipid structures and pores, will be much slower in gel-state membranes than in fluid membranes [45]. Indeed, ITC titrations of POPG vesicles into KLA peptides revealed a very complex binding process (unpublished results), a phenomenon that has also been reported by others [33,46].

The main findings of this study are: (1) the KLA peptides generally show high aggregation power but modest solubilization power, (2) the KLA peptides with low to moderate intrinsic helicity tend to form β-structures and aggregates at high lipid contents (low L/P), (3) the β-structured KLA peptides induce more membrane perturbations as compared with the helical KLA peptides, and (4) the binding affinity of KLA peptides is proportional to the peptides helical propensity and membrane negative surface charge.

ITC titrations were performed to determine quantitatively the effect of the peptide helical propensity and membrane surface properties on the thermodynamics of electrostatic binding to anionic membranes. We analyzed the ITC titration curves using the "one-site" binding model (see Materials and methods section). The surface partitioning model is also commonly used to analyze the titration data and to derive the intrinsic binding factors [47]. For interactions of charged peptides with charged/uncharged lipid membranes, the Gouy–Chapman theory is commonly employed to correct the enhanced/reduced surface concentration of the peptide in comparison to the bulk concentration [32,48–52]. However, due to the substantial amounts of salt and buffer present in the solution that screen the surface charge of the interacting molecules, the influence of the electrostatic attraction/repulsion is minimized so that corrections due to their effects are small [53,54]. Due to the complexity of our system, it is practically impossible to resolve the different sub-processes (e.g. binding, partitioning, conformational changes, pore formation, vesicles solubilization, aggregation), which could take place concurrently during the titration. Therefore, we believe that the use of the one-site binding model, which indeed describes our ITC curves fairly well, to determine the apparent thermodynamic properties of the whole interaction process is sufficient. The one-site binding model was also adequate to describe the binding isotherms in similar systems [36,40,55–57].

The kinetics facet of peptide–lipid membrane interactions is equally important as the interaction thermodynamics [45,58,59]. Generally, the initial binding of the peptides to lipid membranes is almost instantaneous (milliseconds to seconds), a process that is strongly influenced by the membrane physical state, acyl chain length, and surface charge density [60–63]. The peptide dissociation from the membrane is much slower than the association; usually 3–6 orders of magnitude slower [45]. The peptide burial into the lipid bilayer and the subsequent

peptide structural changes and membrane rearrangements will occur on a time scale of milliseconds to seconds [45,63]. The peptide–peptide association and their assembly can take place within seconds [63]. The reorientation of the peptide and lipid molecules in the membrane, the formation of peptide–lipid structures/intermediates, and the formation of peptide or peptide–lipid structural pores are usually slow processes and may need up to hours, which depends on factors like the L/P ratio [45,64–66]. During the ITC, DLS and CD experiments/titrations the peptide–lipid mixtures were only given a few minutes to equilibrate, which is not long enough for the slow insertion and rearrangement processes to take place. In contrast, the samples in the DSC experiments were given much longer time to equilibrate, because of the relatively slow scanning rate, and therefore profound membrane perturbations were observed in the DSC thermograms.

During the ITC titrations, we expect the unordered KLA peptides to form α-helices proportional to their intrinsic helicity. However, the low L/P ratios achieved at the beginning of the ITC titrations will also cause some of the peptides with the low intrinsic helicity to irreversibly adopt β-sheet structures and aggregates. It will be of high interest to determine the (maximum) amount of bound peptide per lipid or liposome. However, this might not be technically feasible because the conformation and binding of KLA peptides are highly sensitive to the preparation procedure, experimental conditions, and the used technique, all of which will affect the resulted peptide-lipid complex. In addition, the formation of the peptide–lipid complex and liposome aggregates is driven by non-covalent bonding and is therefore reversible (see DLS and ITC data) and any attempts to separate the aggregates may drive their dissociation or change their properties. These analyses are plausible when the peptide is covalently linked to the liposome surface [67].

The binding of KLA peptides to DPPG is mainly entropy driven as only a small endothermic binding enthalpy is observed. The entropic part is due to the increase in the rotational and translational degrees of freedom of water molecules upon the desolvation of the hydrophobic residues of the interacting molecules and the liberation of water from the charged residues. Such behavior is explained in literature by the classical hydrophobic effects [68]. Earlier studies of similar systems also revealed mostly entropy driven interactions [32,49,50,55,57]. However, enthalpy driven interactions were also encountered in some other cases [69].

For peptide-lipid interactions, it was found before that up to 60% of ΔG° comes from the exothermic membrane-induced conformational changes of peptides [51,69–73]. The exothermic enthalpy associated with the formation of β-structures is usually smaller than that associated with the formation of α-helices [73]. A better peptide structuring will increase the exothermic enthalpy contribution and will improve the peptide affinity to the membrane. A stronger binding to lipid membranes is associated with the release of more water molecules, which increases the favorable entropic part. It is expected that these phenomena also apply to KLA peptides. It is clear from the ITC data that helical peptides bind stronger to anionic membranes than β-structures, which concurs with earlier observations [74], and that the binding is enhanced with helicity. One explanation can be that helical peptides interact better with membranes than β-sheets. It is also possible that the peptide–peptide interactions during the formation of β-structures will hamper peptide–lipid interactions.

Despite the large amount of exothermic energy liberated upon the conformational changes of the peptides, the experimentally observed ITC isotherms are moderately endothermic. Therefore, we expect the interactions of KLA peptides with lipid bilayers to be also associated with substantial endothermic events that overcompensate the heat release due to the formation of α-helices and β-sheets. Resolving the underlying enthalpy-associated events that take place during the titration of liposomes to KLA peptides is difficult, since what is measured is the net enthalpy change of all the exothermic and endothermic processes. The major exothermic driving forces for the interaction are the non-covalent bonding and membrane partitioning [75,76] as well as the structuring of the KLA peptides [51,69–73]. The profound perturbations upon the burial of the peptides in lipid membranes are endothermic since work must be applied to separate the lipid molecules. Therefore, the thermodynamic profiles are sensitive to the hydrocarbon chain packing in the membrane, i.e. the interaction with well-packed lipid bilayers is associated with a higher endothermic ΔH° [42,50,51,72]. As evident by the high favorable entropy, there will also be high endothermic desolvation energy. Moreover, peptide-induced lipid phase transitions, which will be endothermic, can have a substantial contribution [52]. Processes including vesicles aggregation and solubilization [77], peptide self-association [78], and possible peptide translocation across the bilayer [33,79,80] can also participate to the net ΔH°.

The electrostatic attraction of cationic antimicrobial peptides to the target anionic membranes is the first thermodynamic step in all proposed mechanism of actions of antimicrobial peptides [50]. Both the cationicity of the peptide and the surface charge of the membrane should, in principle, increase the peptide accumulation on the membrane surface. The structuring of the peptides will enhance their incorporation in lipid membranes. Despite the high importance of the peptide helicity and electrostatics in the action of antimicrobial peptides on model lipid membranes, their biological relevance has yet to be verified, as it has been shown before that not all phenomena observed with model membranes are transferable to biological membranes [81,82]. The antimicrobial activity of the KLA peptides was tested before on the Gram-negative *Escherichia coli* (*E. coli*) and the Gram-positive *Staphylococcus epidermidis* (*S. epidermidis*) bacteria (see Table 2) [16,17]. The outer and cytoplasmic membranes of Gram-negative bacteria contain moderate amounts of anionic lipids, typically below 20%, whereas the cytoplasmic membrane of Gram-positive bacteria is rich in anionic lipids, typically more than 50% [12]. The antimicrobial activity of KLA peptides was proportional to their helical propensity, however comparable on both tested species irrespective of their composition and negative charge content. This proposes that in our case study, the peptide helicity is more important than electrostatics for the antimicrobial activity.

Acknowledgments

Dr. Hauke Lilie and Dr. Konstantin Kuppe (Institute of Biochemistry/Biotechnology, Martin-Luther-University Halle-Wittenberg) are gratefully acknowledged for their assistance with the CD measurements. This project was financially supported by the Deutsche Forschungsgemeinschaft through the Graduiertenkolleg "Conformational Transitions in Macromolecular Interactions" (GRK 1026).

References

[1] B. Spellberg, R. Guidos, D. Gilbert, J. Bradley, H.W. Boucher, W.M. Scheld, J.G. Bartlett, J. Edwards, The epidemic of antibiotic-resistant infections: a call to action for the medical community from the infectious diseases society of america, Clinical Infectious Diseases 46 (2008) 155–164.
[2] Extending the Cure, Policy Responses to the Growing Threat of Antibiotic Resistance, Policy Brief 6: The Antibiotic Pipeline, May 2008. , available at http://www.extendingthecure.org/downloads/policy_briefs/Policy_Brief6_May08_newdrugs.pdf.
[3] A. Parisien, B. Allain, J. Zhang, R. Mandeville, C.Q. Lan, Novel alternatives to antibiotics: bacteriophages, bacterial cell wall hydrolases, and antimicrobial peptides, Journal of Applied Microbiology 104 (2008) 1–13.
[4] M. Dathe, T. Wieprecht, Structural features of helical antimicrobial peptides: their potential to modulate activity on model membranes and biological cells, Biochimica et Biophysica Acta 1462 (1999) 71–87.
[5] I. Zelezetsky, A. Tossi, Alpha-helical antimicrobial peptides—using a sequence template to guide structure–activity relationship studies, Biochimica et Biophysica Acta 1758 (2006) 1436–1449.
[6] B. Bechinger, K. Lohner, Detergent-like actions of linear amphipathic cationic antimicrobial peptides, Biochimica et Biophysica Acta 1758 (2006) 1529–1539.
[7] M.R. Yeaman, N.Y. Yount, Mechanisms of antimicrobial peptide action and resistance, Pharmacological Reviews 55 (2003) 27–55.
[8] K.A. Brogden, Antimicrobial peptides: pore formers or metabolic inhibitors in bacteria? Nature Reviews Microbiology 3 (2005) 238–250.

[9] A. Arouri, M. Dathe, A. Blume, Peptide induced demixing in PG/PE lipid mixtures: a mechanism for the specificity of antimicrobial peptides towards bacterial membranes? Biochimica et Biophysica Acta 1788 (2009) 650–659.
[10] R.M. Epand, R.F. Epand, Lipid domains in bacterial membranes and the action of antimicrobial agents, Biochimica et Biophysica Acta 1788 (2009) 289–294.
[11] R.M. Epand, R.F. Epand, Bacterial membrane lipids in the action of antimicrobial agents, Journal of Peptide Science 17 (2011) 298–305.
[12] K. Lohner, E. Sevcsik, G. Pabst, A.L. Liu, Liposome-based biomembrane mimetic systems: implications for lipid–peptide interactions, Advances in Planar Lipid Bilayers and Liposomes 6 (2008) 103–137.
[13] K. Lohner, New strategies for novel antibiotics: peptides targeting bacterial cell membranes, General Physiology and Biophysics 28 (2009) 105–116.
[14] B. Bechinger, Insights into the mechanisms of action of host defence peptides from biophysical and structural investigations, Journal of Peptide Science 17 (2011) 306–314.
[15] V. Teixeira, M.J. Feio, M. Bastos, Role of lipids in the interaction of antimicrobial peptides with membranes, Progress in Lipid Research 51 (2012) 149–177.
[16] M. Dathe, M. Schumann, T. Wieprecht, A. Winkler, M. Beyermann, E. Krause, K. Matsuzaki, O. Murase, M. Bienert, Peptide helicity and membrane surface charge modulate the balance of electrostatic and hydrophobic interactions with lipid bilayers and biological membranes, Biochemistry 35 (1996) 12612–12622.
[17] M. Dathe, T. Wieprecht, H. Nikolenko, L. Handel, W.L. Maloy, D.L. MacDonald, M. Beyermann, M. Bienert, Hydrophobicity, hydrophobic moment and angle subtended by charged residues modulate antibacterial and haemolytic activity of amphipathic helical peptides, FEBS Letters 403 (1997) 208–212.
[18] M. Dathe, J. Meyer, M. Beyermann, B. Maul, C. Hoischen, M. Bienert, General aspects of peptide selectivity towards lipid bilayers and cell membranes studied by variation of the structural parameters of amphipathic helical model peptides, Biochimica et Biophysica Acta 1558 (2002) 171–186.
[19] E. Krause, M. Beyermann, M. Dathe, S. Rothemund, M. Bienert, Location of an amphipathic alpha-helix in peptides using reversed-phase HPLC retention behavior of D-amino acid analogs, Analytical Chemistry 67 (1995) 252–258.
[20] A. Arouri, Interaction of antimicrobial peptides with model lipid membranes. PhD thesis Institute of Chemistry, Martin-Luther-University Halle-Wittenberg, Halle, 2009.
[21] A. Arouri, A. Kerth, M. Dathe, A. Blume, The binding of an amphipathic peptide to lipid monolayers at the air/water interface is modulated by the lipid headgroup structure, Langmuir 27 (2011) 2811–2818.
[22] A. Erbe, A. Kerth, M. Dathe, A. Blume, Interactions of KLA amphipathic model peptides with lipid monolayers, ChemBioChem 10 (2009) 2884–2892.
[23] A.A. Strömstedt, L. Ringstad, A. Schmidtchen, M. Malmsten, Interaction between amphiphilic peptides and phospholipid membranes, Current Opinion in Colloid and Interface Science 15 (2010) 467–478.
[24] A. Arouri, V. Kiessling, L. Tamm, M. Dathe, A. Blume, Morphological changes induced by the action of antimicrobial peptides on supported lipid bilayers, The Journal of Physical Chemistry. B 115 (2011) 158–167.
[25] Y.H. Chen, J.T. Yang, H.M. Martinez, Determination of the secondary structures of proteins by circular dichroism and optical rotatory dispersion, Biochemistry 11 (1972) 4120–4131.
[26] S.W. Provencher, CONTIN: a general purpose constrained regularization program for inverting noisy linear algebraic and integral equations, Computer Physics Communications 27 (1982) 229–242.
[27] G. Zandomeneghi, M.R. Krebs, M.G. McCammon, M. Fandrich, FTIR reveals structural differences between native beta-sheet proteins and amyloid fibrils, Protein Science 13 (2004) 3314–3321.
[28] A. Arouri, O.G. Mouritsen, Anticancer double lipid prodrugs: liposomal preparation and characterization, Journal of Liposome Research 21 (2011) 296–305.
[29] M.M. Domingues, P.S. Santiago, M.A. Castanho, N.C. Santos, What can light scattering spectroscopy do for membrane-active peptide studies? Journal of Peptide Science 14 (2008) 394–400.
[30] J.E. Cummings, T.K. Vanderlick, Aggregation and hemi-fusion of anionic vesicles induced by the antimicrobial peptide cryptdin-4, Biochimica et Biophysica Acta 1768 (2007) 1796–1804.
[31] C. Schwieger, A. Blume, Interaction of poly(L-lysines) with negatively charged membranes: an FT-IR and DSC study, European Biophysics Journal 36 (2007) 437–450.
[32] S. Wen, M. Majerowicz, A. Waring, F. Bringezu, Dicynthaurin (ala) monomer interaction with phospholipid bilayers studied by fluorescence leakage and isothermal titration calorimetry, The Journal of Physical Chemistry. B 111 (2007) 6280–6287.
[33] H. Binder, G. Lindblom, Charge-dependent translocation of the Trojan peptide penetratin across lipid membranes, Biophysical Journal 85 (2003) 982–995.
[34] G. Klocek, J. Seelig, Melittin interaction with sulfated cell surface sugars, Biochemistry 47 (2008) 2841–2849.
[35] T. Lundback, T. Hard, Salt dependence of the free energy, enthalpy, and entropy of nonsequence specific DNA binding, Journal of Physical Chemistry 100 (1996) 17690–17695.
[36] F. Zhang, E.S. Rowe, Calorimetric studies of the interactions of cytochrome c with dioleoylphosphatidylglycerol extruded vesicles: ionic strength effects, Biochimica et Biophysica Acta 1193 (1994) 219–225.
[37] S.K. Kandasamy, R.G. Larson, Effect of salt on the interactions of antimicrobial peptides with zwitterionic lipid bilayers, Biochimica et Biophysica Acta 1758 (2006) 1274–1284.
[38] A. Arouri, P. Garidel, W. Kliche, A. Blume, Hydrophobic interactions are the driving force for the binding of peptide mimotopes and Staphylococcal protein A to recombinant human IgG1, European Biophysics Journal 36 (2007) 647–660.
[39] M.T. Record Jr., C.F. Anderson, T.M. Lohman, Thermodynamic analysis of ion effects on the binding and conformational equilibria of proteins and nucleic acids: the roles of ion association or release, screening, and ion effects on water activity, Quarterly Reviews of Biophysics 11 (1978) 103–178.
[40] E. Goncalves, E. Kitas, J. Seelig, Binding of oligoarginine to membrane lipids and heparan sulfate: structural and thermodynamic characterization of a cell-penetrating peptide, Biochemistry 44 (2005) 2692–2702.
[41] S. Keller, H. Heerklotz, N. Jahnke, A. Blume, Thermodynamics of lipid membrane solubilization by sodium dodecyl sulfate, Biophysical Journal 90 (2006) 4509–4521.
[42] T. Wieprecht, O. Apostolov, J. Seelig, Binding of the antibacterial peptide magainin 2 amide to small and large unilamellar vesicles, Biophysical Chemistry 85 (2000) 187–198.
[43] A. Tossi, L. Sandri, A. Giangaspero, Amphipathic, alpha-helical antimicrobial peptides, Biopolymers 55 (2000) 4–30.
[44] V. Frecer, QSAR analysis of antimicrobial and haemolytic effects of cyclic cationic antimicrobial peptides derived from protegrin-1, Bioorganic & Medicinal Chemistry 14 (2006) 6065–6074.
[45] J.M. Sanderson, Resolving the kinetics of lipid, protein and peptide diffusion in membranes, Molecular and Membrane Biology 29 (2012) 118–143.
[46] C. Schwieger, A. Blume, Interaction of poly(L-arginine) with negatively charged DPPG membranes: calorimetric and monolayer studies, Biomacromolecules 10 (2009) 2152–2161.
[47] U. Schote, P. Ganz, A. Fahr, J. Seelig, Interactions of cyclosporines with lipid membranes as studied by solid-state nuclear magnetic resonance spectroscopy and high-sensitivity titration calorimetry, Journal of Pharmaceutical Sciences 91 (2002) 856–867.
[48] E. Breukink, P. Ganz, B. de Kruijff, J. Seelig, Binding of Nisin Z to bilayer vesicles as determined with isothermal titration calorimetry, Biochemistry 39 (2000) 10247–10254.
[49] F. Bringezu, S. Wen, S. Dante, T. Hauss, M. Majerowicz, A. Waring, The insertion of the antimicrobial peptide dicynthaurin monomer in model membranes: thermodynamics and structural characterization, Biochemistry 46 (2007) 5678–5686.
[50] J. Seelig, Thermodynamics of lipid–peptide interactions, Biochimica et Biophysica Acta 1666 (2004) 40–50.
[51] T. Wieprecht, M. Beyermann, J. Seelig, Thermodynamics of the coil-alpha-helix transition of amphipathic peptides in a membrane environment: the role of vesicle curvature, Biophysical Chemistry 96 (2002) 191–201.
[52] T. Wieprecht, J. Seelig, Isothermal titration calorimetry for studying interactions between peptides and lipid membranes, in: A.S. Sidney, J.M. Thomas (Eds.), Current Topics in Membranes, vol. 52, Academic Press, Amsterdam; Waltham, MA, 2002, pp. 31–56.
[53] G. Cevc, Membrane electrostatics, Biochimica et Biophysica Acta 1031 (1990) 311–382.
[54] M. Langner, K. Kubica, The electrostatics of lipid surfaces, Chemistry and Physics of Lipids 101 (1999) 3–35.
[55] T. Abraham, R.N. Lewis, R.S. Hodges, R.N. McElhaney, Isothermal titration calorimetry studies of the binding of a rationally designed analogue of the antimicrobial peptide gramicidin S to phospholipid bilayer membranes, Biochemistry 44 (2005) 2103–2112.
[56] T. Abraham, R.N. Lewis, R.S. Hodges, R.N. McElhaney, Isothermal titration calorimetry studies of the binding of the antimicrobial peptide gramicidin S to phospholipid bilayer membranes, Biochemistry 44 (2005) 11279–11285.
[57] V.V. Andrushchenko, M.H. Aarabi, L.T. Nguyen, E.J. Prenner, H.J. Vogel, Thermodynamics of the interactions of tryptophan-rich cathelicidin antimicrobial peptides with model and natural membranes, Biochimica et Biophysica Acta 1778 (2008) 1004–1014.
[58] M. Zorko, U. Langel, Cell-penetrating peptides: mechanism and kinetics of cargo delivery, Advanced Drug Delivery Reviews 57 (2005) 529–545.
[59] P.F. Almeida, A. Pokorny, Mechanisms of antimicrobial, cytolytic, and cell-penetrating peptides: from kinetics to thermodynamics, Biochemistry 48 (2009) 8083–8093.
[60] T.D. Bradrick, A. Philippetis, S. Georghiou, Stopped-flow fluorometric study of the interaction of melittin with phospholipid bilayers: importance of the physical state of the bilayer and the acyl chain length, Biophysical Journal 69 (1995) 1999–2010.
[61] I. Constantinescu, M. Lafleur, Influence of the lipid composition on the kinetics of concerted insertion and folding of melittin in bilayers, Biochimica et Biophysica Acta 1667 (2004) 26–37.
[62] K.M. Sekharam, T.D. Bradrick, S. Georghiou, Kinetics of melittin binding to phospholipid small unilamellar vesicles, Biochimica et Biophysica Acta 1063 (1991) 171–174.
[63] J. Tang, H. Yin, J. Qiu, M.J. Tucker, W.F. DeGrado, F. Gai, Using two fluorescent probes to dissect the binding, insertion, and dimerization kinetics of a model membrane peptide, Journal of the American Chemical Society 131 (2009) 3816–3817.
[64] S.M. Ennaceur, M.R. Hicks, C.J. Pridmore, T.R. Dafforn, A. Rodger, J.M. Sanderson, Peptide adsorption to lipid bilayers: slow processes revealed by linear dichroism spectroscopy, Biophysical Journal 96 (2009) 1399–1407.
[65] A.S. Ladokhin, S.H. White, Interfacial folding and membrane insertion of a designed helical peptide, Biochemistry 43 (2004) 5782–5791.
[66] Z. Ningsih, M.A. Hossain, J.D. Wade, A.H. Clayton, M.L. Gee, Slow insertion kinetics during interaction of a model antimicrobial peptide with unilamellar phospholipid vesicles, Langmuir 28 (2012) 2217–2224.
[67] V.P. Torchilin, R. Rammohan, V. Weissig, T.S. Levchenko, TAT peptide on the surface of liposomes affords their efficient intracellular delivery even at low temperature and in the presence of metabolic inhibitors, Proceedings of the National Academy of Sciences of the United States of America 98 (2001) 8786–8791.

[68] S.H. White, W.C. Wimley, Hydrophobic interactions of peptides with membrane interfaces, Biochimica et Biophysica Acta 1376 (1998) 339–352.
[69] T. Wieprecht, O. Apostolov, M. Beyermann, J. Seelig, Membrane binding and pore formation of the antibacterial peptide PGLa: thermodynamic and mechanistic aspects, Biochemistry 39 (2000) 442–452.
[70] A. Bhunia, P.N. Domadia, S. Bhattacharjya, Structural and thermodynamic analyses of the interaction between melittin and lipopolysaccharide, Biochimica et Biophysica Acta 1768 (2007) 3282–3291.
[71] T. Wieprecht, O. Apostolov, M. Beyermann, J. Seelig, Thermodynamics of the alpha-helix-coil transition of amphipathic peptides in a membrane environment: implications for the peptide-membrane binding equilibrium, Journal of Molecular Biology 294 (1999) 785–794.
[72] T. Wieprecht, O. Apostolov, M. Beyermann, J. Seelig, Interaction of a mitochondrial presequence with lipid membranes: role of helix formation for membrane binding and perturbation, Biochemistry 39 (2000) 15297–15305.
[73] M. Meier, J. Seelig, Length dependence of the coil <−−> beta-sheet transition in a membrane environment, Journal of the American Chemical Society 130 (2008) 1017–1024.
[74] G. Klocek, T. Schulthess, Y. Shai, J. Seelig, Thermodynamics of melittin binding to lipid bilayers. Aggregation and pore formation, Biochemistry 48 (2009) 2586–2596.
[75] P. Hoyrup, J. Davidsen, K. Jorgensen, Lipid membrane partitioning of lysolipids and fatty acids: effects of membrane phase structure and detergent chain length, The Journal of Physical Chemistry. B 105 (2001) 2649–2657.
[76] V. Vivcharuk, Y.N. Kaznessis, Thermodynamic analysis of protegrin-1 insertion and permeation through a lipid bilayer, The Journal of Physical Chemistry. B 115 (2011) 14704–14712.
[77] P. Garidel, A. Hildebrand, K. Knauf, A. Blume, Membranolytic activity of bile salts: influence of biological membrane properties and composition, Molecules 12 (2007) 2292–2326.
[78] F. Zehender, A. Ziegler, H.J. Schonfeld, J. Seelig, Thermodynamics of protein self-association and unfolding. The case of apolipoprotein A-I, Biochemistry 51 (2012) 1269–1280.
[79] H. Heerklotz, J. Seelig, Leakage and lysis of lipid membranes induced by the lipopeptide surfactin, European Biophysics Journal 36 (2007) 305–314.
[80] A.N. McKeown, J.L. Naro, L.J. Huskins, P.F. Almeida, A thermodynamic approach to the mechanism of cell-penetrating peptides in model membranes, Biochemistry 50 (2011) 654–662.
[81] A. Arouri, O.G. Mouritsen, Membrane-perturbing effect of fatty acids and lysolipids, Progress in Lipid Research 52 (2013) 130–140.
[82] M.L. Gee, M. Burton, A. Grevis-James, M.A. Hossain, S. McArthur, E.A. Palombo, J.D. Wade, A.H.A. Clayton, Imaging the action of antimicrobial peptides on living bacterial cells, Scientific Reports 3 (2013).